Finding decodable information that is read out in behaviour

Tijl Grootswagers[1,2,3,*] (tijl.grootswagers@sydney.edu.au)

Radoslaw M. Cichy[4] (rmcichy@zedat.fu-berlin.de)

Thomas A. Carlson[1,2] (thomas.carlson@sydney.edu.au)

[1]School of Psychology, University of Sydney, NSW 2006, Australia

[2]ARC Centre of Excellence in Cognition and its Disorders, 16 University Avenue, NSW 2109, Australia

[3]Department of Cognitive Science, Macquarie University, 16 University Avenue, NSW 2109, Australia

[4]Department of Education and Psychology, Freie Universität Berlin, Habelschwerdter Allee 45, 14195, Berlin, Germany

*corresponding author:

School of Psychology, University of Sydney, NSW 2006, Australia

tijl.grootswagers@sydney.edu.au

Keywords: MVPA, decoding, fMRI, behaviour, visual object recognition

Abstract

Multivariate decoding methods applied to neuroimaging data have become the standard in cognitive neuroscience for unravelling statistical dependencies between brain activation patterns and experimental conditions. The current challenge is to demonstrate that information decoded as such by the experimenter is in fact used by the brain itself to guide behaviour. Here we demonstrate a promising approach to do so in the context of neural activation during object perception and categorisation behaviour. We first localised decodable information about visual objects in the human brain using a spatially-unbiased multivariate decoding analysis. We then related brain activation patterns to behaviour using a machine-learning based extension of signal detection theory. We show that while there is decodable information about visual category throughout the visual brain, only a subset of those representations predicted categorisation behaviour, located mainly in anterior ventral temporal cortex. Our results have important implications for the interpretation of neuroimaging studies, highlight the importance of relating decoding results to behaviour, and suggest a suitable methodology towards this aim.

Significance statement

Brain decoding methods are a powerful way to analyse neuroimaging data. An implicit assumption in many decoding studies is that when information can be decoded, then the brain is using this information for behaviour. However, this assumption must be explicitly tested. Here, using visual object categorisation as an example, we separately localised decodable information and information that can be used to predict behaviour. Our findings showed that only from a subset of areas that had decodable category information, we could predict observer categorisation reaction times. Our results highlight the distinction between decodable information and information that is suitably formatted for read-out by the brain in behaviour. Our results have critical implications for the interpretation of decoding studies in general.

1 Introduction

Multivariate pattern analysis (MVPA), also called brain decoding, are a powerful tool to establish statistical dependencies between experimental conditions and brain activation patterns measured with functional Magnetic Resonance Imaging (fMRI) (1–7). An implicit assumption often made by the experimenters conducting such analyses is that if information can be decoded, then this information is available to the brain to use in behaviour (8, 9). However, this does not have to be the case, as it could be that the decoded information is different from the signal that is relevant for the brain (8, 10). For example, the decodable information could be epiphenomenal, or the information could be used for a different behaviour than stipulated (cf. 11). Thus, a current challenge in cognitive neuroscience is to relate the decoded information to behaviour. Previous work has approached this issue by, for example, correlating classifier performances to behavioural accuracies (10, 12–17). However, this does not establish the link between brain responses and behaviour at the level of individual experimental conditions. Another approach has been to link behaviour and brain patterns through common similarity structure: if two stimuli evoke similar brain responses, and elicit similar behaviour, brain responses and behaviour are to be linked (18–25). While this approach does link behaviour and brain patterns at the level of single experimental conditions, it is unclear whether the link established such carries over to decision making behaviour such as categorisation.

Recently, a novel methodological approach, called the distance-to-bound approach, has been proposed (26, 27). This method promises to form a tight link between brain activity and behaviour by connecting brain responses at the level of individual experimental conditions directly to perceptual decision-making behaviour. The rationale behind the distance-to-bound approach (16, 26–28) is that in a decision-making task, the brain applies a linear read out process (29) to a neural activation space. Similarly, classifiers in decoding studies fit multi-dimensional hyperplanes to

separate a neural activation space into separate classes. If the neural activation space used for the decision-making task is the same space that is used by the classifier in a decoding study, then the classifier's decision hyperplane can be interpreted as an observer's decision boundary for the decision-making task. Analogous to the prediction of signal detection theory for the univariate case, in the multivariate space, the closer the input is to the decision boundary, the more ambiguous the evidence for the decision (30). Thus, if for a decision task (e.g., categorisation), the brain uses the same information as the MVPA classifier, then the distance to the classifier hyperplane reflects the ambiguity of the evidence for the decision. Ambiguous evidence in turn predicts longer reaction times (31, 32), and therefore distance to the classifier hyperplane is predicted to negatively correlate with reaction time.

First studies employing the distance-to-boundary approach have demonstrated its promise in a region of interest based approach using fMRI (27), and a time-varying approach using MEG (33, 34). Here, we go beyond those studies by using the distance-to-boundary approach to separately localise information that is decodable, and information that is suitably formatted for read out by the brain. We did not limit our analysis to specific regions of interest, but we used a spatially unbiased approach to create maps of where in the brain information can be used to guide behaviour.

2 Results

We examined the relationship between decodable information and information that is suitably formatted for read-out by the brain in the context of decodable information about visual objects and object categorisation behaviour.

To ensure robustness and generality of our results, we analysed in parallel two independent fMRI datasets (35, 36), with different stimulus sets, and in relation to partly overlapping categorisation behaviours. Stimuli for experiment 1 consisted of animate and inanimate objects (Figure 1A). The animate objects could be further divided into faces, bodies, humans and animals. The stimuli for experiment 2 consisted of 118 visual objects (Figure 1C), which could also be divided into 27 animate and 91 inanimate objects. The inanimate objects were further subdivided into tools, food, and transport objects. Overall, this allowed us to investigate the relationship between decodable information from brain activity and categorisation behaviour for six different distinctions: animate versus inanimate, faces versus bodies, human versus animal, tools versus not tools, food versus not food, and transport versus not food. Note that the negative 'not-X' category was defined as all stimuli that did fall into one of the aforementioned classes.

After collecting human categorisation reaction times (Figure 1E) for each of the six categorical distinctions, we determined the relationship between decodable information and behaviour for each of the six distinctions separately as follows (Fig. 1F). First, we determined where information about objects is present in brain patterns using decoding in a standard fMRI searchlight decoding analysis (6, 37). In detail, at each spatial location (voxel) in an fMRI image, a support vector machine (SVM) was used to classify visual object category based on local brain patterns, resulting in a map of classification accuracies.

We then determined the subset of the locations at which brain patterns were suitably formatted for read-out by the brain using the distance-to-bound approach (26) in a second searchlight analysis. Analogous to the decoding analysis, at each voxel, an SVM was trained to classify visual objects. Diverging at this point from the decoding approach we did not test the classifier, but rather obtained the distance for each exemplar to the hyperplane set by the SVM. We then

correlated those distances to reaction times acquired in separate categorisation tasks (Fig. 1E). A separate correlation was computed for the two categories in the task. Conducted for every fMRI subject (N=15), this resulted in subject-specific maps of voxels containing object information, and maps of voxels with information that is suitably formatted for readout in a categorisation task. Both sets of maps were subjected to inference statistics at the group level using one-sided sign rank tests and thresholded at $p < 0.05$ (fdr-corrected for multiple comparisons across voxels).

***** Figure 1 *****

2.1 A subset of locations that have decodable information about animacy also had information suitably formatted for animacy categorisation behaviour

Animacy is a pervasive and basic object property according to which any object can be classified as animate or inanimate (38). Previous studies have shown that the division of animate versus inanimate objects is reflected in the large-scale architecture of high-level visual areas such as the ventral temporal cortex (VTC) (38–40), However, it has also been shown that animacy can be decoded not only from VTC, but from the whole ventral visual stream (36, 40, 41). Furthermore, categorical object responses have also been found in the dorsal visual stream (42–44) and in frontal areas (45, 46). This prompts the question of where in the visual system object representations are suitably formatted for read-out by the brain for animacy decisions.

Corroborating previous studies, we found decodable information about animacy in the entire ventral visual stream from the occipital pole to anterior ventral temporal cortex (Figure 2AB, Table 1AD, N = 15, one-sided sign-rank test, $p < 0.05$ fdr-corrected). In addition, we found decodable information in dorsal and prefrontal cortex (Figure 2B) in experiment 2 which had full brain coverage. Localising the brain representations suitable to guide animacy categorisation behaviour

148 (using the distance-to-bound approach) revealed convergent evidence across experiments that
149 only a subset of voxels containing decodable information fulfilled this criterion. In detail, distance-
150 RT-correlations for animate objects were strongest in the high-level regions of the ventral and the
151 dorsal stream (Table 1). For inanimate objects, we found no voxels with significant distance-RT-
152 correlations (cf. 27, 34).
153
154 ***** Figure 2 *****
155
156 **2.2 The proportion of region-specific representations suitably formatted for behaviour increases**
157 **along the ventral stream and decreases along the dorsal stream**
158 We next explicitly determined the degree to which representations in single brain regions within
159 the ventral and dorsal streams are suitably formatted for behaviour. For this we parcellated the
160 cortex (Figure 3A) using a probabilistic topographic map of visual processing areas (47). For each
161 region, we calculated the ratio between the number of significant voxels in the decoding analysis
162 and the total number of voxels, so that a high ratio indicates that a large part of a region contains
163 object representations with categorical information. Similarly, we calculated the ratio between the
164 number of significant voxels in the distance-to-bound analysis and the total number of voxels.
165 Here, a high ratio indicates that a large part of a region contains object representations that are
166 suitably formatted for read out in a categorisation task.
167
168 In the ventral stream, we observed a systematic increase in ratio with processing stage, from early
169 visual areas to high-level visual areas, with highest ratios in ventral occipital (VO) and
170 parahippocampal (PHC) cortex (Figure 3 B&C). In contrast, in the dorsal stream we observed a
171 systematic decrease of the correlation ratio with processing stage. In addition, significant animacy
172 decoding information was found in similar proportions in the ventral-temporal areas as in lateral-

occipital areas, however, the proportion of voxels with information suitable for categorisation was lower in lateral-occipital areas. This is consistent with the notion that while both these regions contain object representations, the VTC contains location-invariant representations which are essential for object categorisation (10, 24, 48, 49).

In sum, these results show that representations along the ventral stream are shaped for optimal read-out of categorical information (40, 49). In contrast, representations in the dorsal stream might be shaped for the read-out in different tasks (17, 43). These results also suggest that intermediate stages along the ventral and dorsal streams may be similar or partly shared, as suggested by the similar ratios of information suitable for read-out.

***** Figure 3 *****

2.3 Decodable information about subordinate categorisation tasks is also suitably formatted for categorisation behaviour

While animacy categorisation may be based on large-scale representational differences in the visual brain (39, 40, 50, 51), subordinate categorisation tasks (e.g., faces, bodies, tools) may depend more on fine grained patterns in focal brain regions (52–54). Here, we tested whether decodable information about subordinate category membership is also suitably formatted for read out in respective categorisation tasks. We tested two subordinate contrasts for experiment 1: face versus body, and human versus animal using the same general procedure as for animacy. We found that both contrasts were decodable (Table 1B-C). We found a significant correlation between distance to the classifier hyperplane and reaction time for faces in the face versus body task (Figure 4A). Of the subordinate categorisation contrasts in experiment 2 (food, transport or tool versus everything else), transport and tool versus everything else were not significantly

198 decodable information nor had they significant correlations (Table 1E-F). Food versus not food
199 resulted in significant decodable information, and significant distance-RT correlations were
200 present for this contrast in the 'not food' category (Figure 4B, Table 1G). Taken together, for some
201 subordinate categorisation contrasts that were decodable, we were successful in localising brain
202 patterns suitably formatted for read-out in behaviour.
203
204 ***** Figure 4 *****
205
206 ***** Table 1 *****
207
208 **3 Discussion**
209 **3.1 Summary**
210 The aim of this study was to examine where in the brain decodable information is suitably
211 formatted for read-out by the brain in behaviour. We found that only a subset of information that
212 is decodable could be related more directly to behaviour using the distance-to-bound approach,
213 which argues for a partial dissociation between decodable information and information that is
214 relevant for behaviour. Besides high-level ventral visual cortex (29, 55, 56), mid-level visual stream
215 (V3 & hV4) and dorsal stream (IPS) regions harboured representations that are formatted suitable
216 to guide behaviour.
217
218 **3.2 Dissociating between decodable information and information that is used in behaviour**
219 Our results speak to a current challenge in neuroimaging, which is to show that information visible
220 to the experimenter is in fact read out by the brain. By showing that only a subset of decodable
221 category information correlates with independent observer categorisation RTs, we demonstrate a
222 dissociation between information that is decodable, and information related to behaviour. To

223 illustrate, consider the question about what regions are used by the brain to perform an object
224 animacy categorisation task (40, 55). When only the result of the animacy decoding searchlight
225 would be taken into account, this might be interpreted as meaning that the brain may use
226 animacy information from anywhere in the ventral stream in animacy categorisation. However,
227 when testing this interpretation directly using the distance-RT-correlation results, it becomes clear
228 that object animacy information is represented for read-out in mid- and high-level visual areas
229 only (9, 10).
230
231 It is important to note that not finding a correlation between distance to the classifier hyperplane
232 and RT does not imply this information is necessarily irrelevant or epiphenomenal. For example, it
233 could be that the representations are relevant for a task other than the binary categorisation
234 decision that was used here, or that other read-out models provide a better description (e.g., non-
235 linear models (26)). Therefore, the current approach only allows the positive inference on the level
236 of suitability of decoded information in the context of a limited set of tasks, and a limited set of
237 read-out models. While a correlation with behaviour still does not imply that the information is
238 used by the brain, it shows that the information is formatted in a way that is suitable to be used by
239 the brain for decisions (8–10, 56).
240
241 **3.3 The contribution of ventral and dorsal visual regions to categorisation behaviour**
242 We found that neural representations suitably formatted for behaviour in categorisation were
243 most prominently located in the anterior regions of the VTC. This corroborates previous studies
244 (27, 57–59), and reinforces the tight link between VTC and visual categorisation behaviour.
245
246 However, we found that correlations between distance to boundary and RT were not restricted to
247 anterior regions of the VTC, but were also prominent in V3 and hV4 (Figure 2) as well. This

248 suggests that representations in these areas are suitable for read-out. This is consistent with the
249 view that lower level visual features as encoded in mid-level visual regions could aid faster read-
250 out of category information. V4 is thought of as an intermediate stage of visual processing that
251 aggregates lower level visual features into invariant representations (60). It has been proposed
252 that a direct pathway from V4 to areas that facilitate eye movements (e.g., FEF) accounts for fast
253 saccadic categorisation reaction times (61, 62). Similar pathways to decision making areas would
254 allow the brain to exploit visual feature cues to enable fast responses to ecologically important
255 stimuli (58, 63, 64). An alternative possibility is that read out is not happening directly from V4,
256 but its representational structure is shaped by the low-level feature differences in animacy. This
257 structure is then largely preserved when it is communicated to more anterior areas. This would
258 explain similar correlations between distance to the classifier boundary and reaction time in both
259 V4, and more anterior areas of the ventral stream. Both of these accounts are consistent with
260 recent findings that show differential responses for object categories in mid-level visual areas
261 based on visual feature differences, such as in animacy (21, 41), or object size (65). The extent to
262 which shape information contributes to the read-out process could be further investigated by
263 using the approach from this study with a stimulus set that controls for these visual features (21,
264 66), or by decoding and predicting reaction times from texture stimuli that have similar features
265 (41).
266
267 Finally, we found that correlations with RT were also present in parietal areas. We found that
268 information in early parietal areas also correlates with RT. The classical view is that the ventral and
269 dorsal visual streams are recruited for different function (67), with the ventral stream representing
270 object identities ('what'), and the dorsal stream spatial features ('where'). However, areas in the
271 dorsal stream, such as IPS1 and IPS2 have been found to exhibit similar object-selective responses
272 as areas in the ventral stream (17, 42, 68, 69). In according with this, we found similar correlations

273 between distance and RT in mid-level areas in the ventral and dorsal streams. However, our
274 results also showed that the proportion of correlations between distance and RT decreased
275 further in the dorsal stream, while they increased in the ventral stream (Figure 4). This suggests
276 that representations in the ventral and dorsal streams undergo similar transformations at first,
277 and then diverge for different goals.
278
279 **3.4 Without a task, neural object representations in the VTC are still formatted for read-out in**
280 **categorisation decisions**
281 In the current study, the fMRI participants performed an orthogonal task at fixation, and were not
282 actively categorising. Despite this, categorisation reaction times could still be predicted from
283 representations in the visual stream. This highlights that, without a task, information in the visual
284 system is represented in a way that is suitable for read out in behaviour (27, 33). In addition, the
285 orthogonal task in the scanner has the advantage that it avoids motor effects and difficulty
286 confounds in the modelling of the BOLD response (70, 71). Future studies might use the distance-
287 to-bound approach with participants actively performing the same task in the scanner, where we
288 predict that areas involved in the decision making and execution processes would contain
289 information that correlates with reaction time. For example, some areas are believed to
290 preferentially represent task-relevant information, such as areas in the prefrontal cortex (72–74),
291 and in the parietal stream (43, 75, 76). In the absence of an animacy categorisation task, one
292 would predict that animacy information would not be strongly represented in these areas. Yet, our
293 results showed that animacy information can be decoded from prefrontal and parietal areas when
294 participants perform an orthogonal task. Thus, only considering the decoding results would
295 suggest that animacy is represented in these areas. However, our results also showed that the
296 animacy information in these areas was not predictive of reaction time. This again highlights the
297 dissociation between information that can be decoded, and information that is suitable for read

out in behaviour. A prediction that follows from this is that performing an active object categorisation task in the scanner would change the representations in these task-relevant areas so that they become predictive of reaction time (77).

3.5 Asymmetric distance-RT-Correlations in binary categorisation tasks

In both experiments, there was evidence for correlations between distance and reaction time for animate stimuli, but none for the inanimate stimuli, consistent with previous work (27, 33, 34). A possible explanation put forward there was that this discrepancy might be the effect of animacy being a negatively defined category (i.e., “not animate”). Under this hypothesis the animacy categorisation task can be performed by collecting evidence for animate stimuli and responding inanimate only when not enough evidence was accumulated after a certain amount of time. Here, we tested a prediction of this hypothesis using contrasts consisting of two positively defined categories, namely human versus animal, and face versus body. We found that for the face versus body contrast there was a distance-RT-correlation only for faces. This goes against the notion of the negative definition of inanimate as the main reason for a lack of correlation. However, it still is possible that observers still treated these tasks as A or NOT A, rather than A or B, while choosing ‘A’ based on the category that is easiest to detect (34). For example, perceptual evidence for a face would be easier to obtain that evidence for a body-part, as faces share low level visual features (62, 78, 79). Thus, while not explicitly specified as a negative category, it could have been treated as such.

This suggest that the binary categorisation might be an unnatural way of approaching human categorisation behaviour in the real world. Other operationalisations may be better suited to capture behaviour (11). This could be investigated further by assessing behaviour in tasks that do

not require binary categorisation, such as picture naming or visual search, and assessing whether in those tasks the distance-to-bound approach can also be used to predict observer behaviour. Still, it is important to note that the binary task matches the brain decoding task performed by the classifier. The above-chance decoding accuracy in the brain decoding task is commonly interpreted as a similar dichotomy in the brain's representation that the brain can use in a decision. However, when only the information in one of the categories (i.e., animals or faces) can be used to predict decision behaviour, as shown here, then this interpretation needs to be revisited.

3.6 Conclusion

In this study, we combined the distance-to-bound approach (26) with a searchlight decoding analysis to find brain areas with decodable information that is suitable for read-out in behaviour. Our results showed that decodable information is not always equally suitable for read-out by the brain in behaviour. This speaks to the current debate in neuroimaging research about whether the information that we can decode is the same information that is used by the brain in behaviour (8).

4 Materials and Methods

The aim of this study was to correlate distance to a classifier's hyperplane to reaction times (RTs) for categorisation. In this section, we describe the stimuli and fMRI data that were obtained from previous experiments (35, 36). Next, we collected categorisation reaction times for those stimuli on Amazon's Mechanical Turk. Finally, we describe the two-step searchlight procedure used to create decoding and correlation maps of areas involved in visual object categorisation.

4.1 Stimuli

We used the stimuli from two experiments that have been published (35, 36). Stimuli for experiment 1 consisted of 92 visual objects, segmented on a white background (Figure 1A). Stimuli

347 consisted of animate and inanimate objects. The animate objects could be further divided into
348 faces, bodies, humans and animals. Inanimate objects consisted of natural (e.g., plants or fruits)
349 and man-made items (e.g., tools or houses). The stimulus set for experiment 2 consisted of 118
350 visual objects on natural backgrounds, shown in Figure 1C. A small proportion of the objects (27)
351 were animate. The inanimate objects included subcategories such as tools, or food items. In both
352 experiments, participants were presented with the visual object stimuli while performing an
353 orthogonal task at fixation. Stimuli were displayed at 2.9° (Experiment 1) and 4.0° (Experiment 2)
354 visual angle with 500 ms duration. Images were displayed (overlaid with a grey fixation cross) for
355 500 ms in random order.
356
357 **4.2 fMRI recordings**
358 The first experiment (35) had high resolution fMRI coverage of the ventral visual stream (Figure
359 1B) from 15 participants with a 2 mm isotropic voxel resolution. The second experiment (36) had
360 whole brain from 15 participants with a 3 mm isotropic voxel resolution. In both experiments, at
361 the start of a session, structural images were obtained using a standard T_1-weighted sequence.
362 fMRI data were aligned and coregistered to the T1 structural image, and then normalized to a
363 standard MNI template. General linear models were used to compute t-values for each stimulus
364 (92 and 118, respectively) against baseline.
365
366 **4.3 Reaction time data**
367 We obtained reaction times for the stimuli in multiple different categorisation contrasts (Figure
368 1A&B). For experiment 1, these were animate versus inanimate, face versus body, and human
369 versus animal. For experiment 2, we tested animate versus inanimate, tool versus not tool, food
370 versus not food, and transport versus not transport. The RTs were collected using Amazons
371 Mechanical Turk (MTurk). For each of the categorisation contrasts, 50 unique participants

372 performed a categorisation task using the same stimuli as were used in collecting the fMRI data.
373 Participants were instructed to "Categorise the images as fast and accurate as possible using the
374 following keys: (z for X, m for Y)", where X and Y would be replaced with the relevant categories
375 (e.g., animate and inanimate) for the contrast. On each trial, an image was presented for 500ms,
376 followed by a black screen until the participant's response (Figure 1C). The presentation order of
377 the stimuli was randomized and stimuli did not repeat. This resulted in 50 reaction time values per
378 exemplar (one for each participant). Each participant's reaction times were z-scored. Next, we
379 computed the median reaction time (across participants) for each exemplar. his resulted in one
380 reaction time value per exemplar, which were used in the rest of the study.
381
382 **4.4 Searchlight procedure**
383 For each categorisation contrast and subject, we used a searchlight approach (6, 37) to create
384 maps of decoding accuracy and of correlations between distance to the classifier boundary and
385 categorisation reaction times. In contrast to pre-defined ROI's, which are used to test a-priori
386 hypotheses about the spatial origin of information in the brain, the searchlight results in a spatially
387 unbiased map of decodable information. An overview of the approach is presented in Figure 1D.
388
389 To create the decoding accuracy maps, we used a standard searchlight decoding approach (4, 6,
390 80, 81), as implemented in the CoSMoMVPA decoding toolbox (82). For each voxel in the three-
391 dimensional fMRI voxel space, t-values belonging to a spherical cluster (4 voxel radius) centred
392 around this voxel were arranged into a vector for each stimulus. The stimuli vectors were then
393 split up into five sets for cross-validation. A support vector machine (SVM) classifier was trained on
394 four sets and its prediction accuracy was tested on the left out set. This was repeated five times,
395 using each set for testing once. The mean accuracy across these repetitions was stored at the
396 centre voxel of the sphere. Repeating the process over all voxels resulted in a 3D-map of decoding

accuracies. The searchlight procedure was conducted for each subject independently, resulting in one accuracy map for each subject for each task.

Next, we created maps of correlations between distance to the classifier hyperplane and observer categorisation reaction times on the same contrast. Vectors of t-values were obtained for each stimulus in the same manner as the first searchlight procedure. Then, an SVM classifier was trained using all the stimuli, effectively fitting a hyperplane that distinguished between vector patterns according to category. We then computed the distance of each exemplar to this decision hyperplane, resulting in one distance value per exemplar. The distance values were rank-order correlated (Spearman's ρ) to the median MTurk reaction times collected in the behavioural experiment for the same exemplars in the analogous categorisation task. The contribution of each category was assessed individually, by performing the correlations separately for the two sides of the categorisation (i.e., one correlation for animate and one for inanimate exemplars). For each categorisation task this resulted in two correlation maps per subject. The maps of decoding accuracy and correlations were assessed for significance at the group level using sign-rank tests for random-effects inference. The results were thresholded at $p<0.05$, using the false discovery rate (FDR; (83)) to correct for multiple comparisons at the voxel level.

4.5 Relating the results to topographical locations of the visual system

For each of the categorisation contrasts, we identified the locations of the significant voxels with respect to ROIs of the visual system. The significant voxels in the decoding maps and correlation maps were compared to probabilistic topographic maps of visual processing areas (47), which represent for each voxel the visual area with the highest probability. A percentage score for each ROI was then computed, reflecting the percentage of voxels in this ROI that were significant at the group level. We obtained a bootstrapped distribution of percentage scores for each ROI by

422 repeating this procedure 10,000 times, while randomly sampling the subjects with replacement
423 and recomputing the group level statistics. We report the 5th, 50th and 95th percentiles of this
424 distribution. This approach allows quantifying the difference between the number of decoding
425 voxels and correlation voxels per visual ROI.

426

427 **Acknowledgements**

428 This research was supported by an Australian Research Council Future Fellowship (FT120100816)
429 and an Australian Research Council Discovery project (DP160101300) awarded to T.A.C., and
430 a German Research Foundation grant (CI-241/1-1) awarded to R.M.C. The authors acknowledge
431 the University of Sydney HPC service for providing High Performance Computing resources.

432

433 **References**

434 1. Carlson TA, Schrater P, He S (2003) Patterns of Activity in the Categorical Representations of
435 Objects. *J Cogn Neurosci* 15(5):704–717.

436 2. Cox DD, Savoy RL (2003) Functional magnetic resonance imaging (fMRI) "brain reading":
437 detecting and classifying distributed patterns of fMRI activity in human visual cortex.
438 *NeuroImage* 19(2):261–270.

439 3. Haxby JV, et al. (2001) Distributed and Overlapping Representations of Faces and Objects in
440 Ventral Temporal Cortex. *Science* 293(5539):2425–2430.

441 4. Haynes J-D (2015) A Primer on Pattern-Based Approaches to fMRI: Principles, Pitfalls, and
442 Perspectives. *Neuron* 87(2):257–270.

443 5. Kamitani Y, Tong F (2005) Decoding the visual and subjective contents of the human brain.
444 *Nat Neurosci* 8(5):679–685.

445 6. Kriegeskorte N, Goebel R, Bandettini P (2006) Information-based functional brain mapping.
446 *Proc Natl Acad Sci U S A* 103(10):3863–3868.

447 7. Tong F, Pratte MS (2012) Decoding Patterns of Human Brain Activity. *Annu Rev Psychol*
448 63(1):483–509.

449 8. de-Wit L, Alexander D, Ekroll V, Wagemans J (2016) Is neuroimaging measuring information
450 in the brain? *Psychon Bull Rev* 23(5):1415–1428.

9. Ritchie JB, Kaplan DM, Klein C (2017) Decoding the Brain: Neural Representation and the Limits of Multivariate Pattern Analysis in Cognitive Neuroscience. *Br J Philos Sci*. doi:10.1093/bjps/axx023.

10. Williams MA, Dang S, Kanwisher NG (2007) Only some spatial patterns of fMRI response are read out in task performance. *Nat Neurosci* 10(6):685–686.

11. Krakauer JW, Ghazanfar AA, Gomez-Marin A, MacIver MA, Poeppel D (2017) Neuroscience Needs Behavior: Correcting a Reductionist Bias. *Neuron* 93(3):480–490.

12. Naselaris T, Kay KN, Nishimoto S, Gallant JL (2011) Encoding and decoding in fMRI. *NeuroImage* 56(2):400–410.

13. Raizada RDS, Tsao F-M, Liu H-M, Kuhl PK (2010) Quantifying the Adequacy of Neural Representations for a Cross-Language Phonetic Discrimination Task: Prediction of Individual Differences. *Cereb Cortex* 20(1):1–12.

14. van Bergen RS, Ji Ma W, Pratte MS, Jehee JFM (2015) Sensory uncertainty decoded from visual cortex predicts behavior. *Nat Neurosci* 18(12):1728–1730.

15. Walther DB, Caddigan E, Fei-Fei L, Beck DM (2009) Natural Scene Categories Revealed in Distributed Patterns of Activity in the Human Brain. *J Neurosci* 29(34):10573–10581.

16. Philiastides MG, Sajda P (2006) Temporal Characterization of the Neural Correlates of Perceptual Decision Making in the Human Brain. *Cereb Cortex* 16(4):509–518.

17. Freud E, Culham JC, Plaut DC, Behrmann M (2017) The large-scale organization of shape processing in the ventral and dorsal pathways. *eLife* 6:e27576.

18. Bracci S, op de Beeck H (2016) Dissociations and Associations between Shape and Category Representations in the Two Visual Pathways. *J Neurosci* 36(2):432–444.

19. Cohen MA, Dennett DC, Kanwisher N (2016) What is the Bandwidth of Perceptual Experience? *Trends Cogn Sci* 20(5):324–335.

20. Mur M, et al. (2013) Human Object-Similarity Judgments Reflect and Transcend the Primate-IT Object Representation. *Front Psychol* 4. doi:10.3389/fpsyg.2013.00128.

21. Proklova D, Kaiser D, Peelen MV (2016) Disentangling Representations of Object Shape and Object Category in Human Visual Cortex: The Animate–Inanimate Distinction. *J Cogn Neurosci*:1–13.

22. Redcay E, Carlson TA (2015) Rapid neural discrimination of communicative gestures. *Soc Cogn Affect Neurosci* 10(4):545–551.

23. Wardle SG, Kriegeskorte N, Grootswagers T, Khaligh-Razavi S-M, Carlson TA (2016) Perceptual similarity of visual patterns predicts dynamic neural activation patterns measured with MEG. *NeuroImage* 132:59–70.

24. Haushofer J, Livingstone MS, Kanwisher N (2008) Multivariate Patterns in Object-Selective Cortex Dissociate Perceptual and Physical Shape Similarity. *PLOS Biol* 6(7):e187.

25. Grootswagers T, Kennedy BL, Most SB, Carlson TA (2017) Neural signatures of dynamic emotion constructs in the human brain. *Neuropsychologia*. doi:10.1016/j.neuropsychologia.2017.10.016.

26. Ritchie JB, Carlson TA (2016) Neural Decoding and "Inner" Psychophysics: A Distance-to-Bound Approach for Linking Mind, Brain, and Behavior. *Front Neurosci*:190.

27. Carlson TA, Ritchie JB, Kriegeskorte N, Durvasula S, Ma J (2014) Reaction Time for Object Categorization Is Predicted by Representational Distance. *J Cogn Neurosci* 26(1):132–142.

28. Kiani R, Cueva CJ, Reppas JB, Newsome WT (2014) Dynamics of Neural Population Responses in Prefrontal Cortex Indicate Changes of Mind on Single Trials. *Curr Biol* 24(13):1542–1547.

29. DiCarlo JJ, Cox DD (2007) Untangling invariant object recognition. *Trends Cogn Sci* 11(8):333–341.

30. Green DM, Swets JA (1966) Signal detection theory and psychophysics. *N Y*.

31. Ashby FG (2000) A Stochastic Version of General Recognition Theory. *J Math Psychol* 44(2):310–329.

32. Ashby FG, Maddox WT (1994) A Response Time Theory of Separability and Integrality in Speeded Classification. *J Math Psychol* 38(4):423–466.

33. Ritchie JB, Tovar DA, Carlson TA (2015) Emerging Object Representations in the Visual System Predict Reaction Times for Categorization. *PLoS Comput Biol* 11(6):e1004316.

34. Grootswagers T, Ritchie JB, Wardle SG, Heathcote A, Carlson TA (2017) Asymmetric Compression of Representational Space for Object Animacy Categorization under Degraded Viewing Conditions. *J Cogn Neurosci* 29(12):1995–2010.

35. Cichy RM, Pantazis D, Oliva A (2014) Resolving human object recognition in space and time. *Nat Neurosci* 17(3):455–462.

36. Cichy RM, Pantazis D, Oliva A (2016) Similarity-Based Fusion of MEG and fMRI Reveals Spatio-Temporal Dynamics in Human Cortex During Visual Object Recognition. *Cereb Cortex N Y N 1991* 26(8):3563–3579.

37. Haynes J-D, et al. (2007) Reading Hidden Intentions in the Human Brain. *Curr Biol* 17(4):323–328.

38. Caramazza A, Shelton JR (1998) Domain-Specific Knowledge Systems in the Brain: The Animate-Inanimate Distinction. *J Cogn Neurosci* 10(1):1–34.

39. Kriegeskorte N, et al. (2008) Matching Categorical Object Representations in Inferior Temporal Cortex of Man and Monkey. *Neuron* 60(6):1126–1141.

40. Grill-Spector K, Weiner KS (2014) The functional architecture of the ventral temporal cortex and its role in categorization. *Nat Rev Neurosci* 15(8):536–548.

41. Long B, Yu C-P, Konkle T (2017) A mid-level organization of the ventral stream. *bioRxiv*:213934.

42. Konen CS, Kastner S (2008) Two hierarchically organized neural systems for object information in human visual cortex. *Nat Neurosci* 11(2):224–231.

43. Bracci S, Daniels N, op de Beeck H (2017) Task Context Overrules Object- and Category-Related Representational Content in the Human Parietal Cortex. *Cereb Cortex*:1–12.

44. Freedman DJ, Assad JA (2006) Experience-dependent representation of visual categories in parietal cortex. *Nature* 443(7107):85–88.

45. Freedman DJ, Riesenhuber M, Poggio T, Miller EK (2001) Categorical Representation of Visual Stimuli in the Primate Prefrontal Cortex. *Science* 291(5502):312–316.

46. Freedman DJ, Riesenhuber M, Poggio T, Miller EK (2003) A Comparison of Primate Prefrontal and Inferior Temporal Cortices during Visual Categorization. *J Neurosci* 23(12):5235–5246.

47. Wang L, Mruczek REB, Arcaro MJ, Kastner S (2015) Probabilistic Maps of Visual Topography in Human Cortex. *Cereb Cortex* 25(10):3911–3931.

48. Schwarzlose RF, Swisher JD, Dang S, Kanwisher N (2008) The distribution of category and location information across object-selective regions in human visual cortex. *Proc Natl Acad Sci* 105(11):4447–4452.

49. Cichy RM, et al. (2013) Probing principles of large-scale object representation: Category preference and location encoding. *Hum Brain Mapp* 34(7):1636–1651.

50. Carlson TA, Tovar DA, Alink A, Kriegeskorte N (2013) Representational dynamics of object vision: The first 1000 ms. *J Vis* 13(10):1.

51. Downing PE, Chan AW-Y, Peelen MV, Dodds CM, Kanwisher N (2006) Domain Specificity in Visual Cortex. *Cereb Cortex* 16(10):1453–1461.

52. Downing PE, Jiang Y, Shuman M, Kanwisher N (2001) A Cortical Area Selective for Visual Processing of the Human Body. *Science* 293(5539):2470–2473.

53. Downing PE, Peelen MV (2016) Body selectivity in occipitotemporal cortex: Causal evidence. *Neuropsychologia* 83:138–148.

54. Kanwisher N, McDermott J, Chun MM (1997) The Fusiform Face Area: A Module in Human Extrastriate Cortex Specialized for Face Perception. *J Neurosci* 17(11):4302–4311.

55. DiCarlo JJ, Zoccolan D, Rust NC (2012) How Does the Brain Solve Visual Object Recognition? *Neuron* 73(3):415–434.

56. Klein C (2016) Brain regions as difference-makers. *Philos Psychol* 0(0):1–14.

57. Afraz S-R, Kiani R, Esteky H (2006) Microstimulation of inferotemporal cortex influences face categorization. *Nature* 442(7103):692–695.

58. Hong H, Yamins DLK, Majaj NJ, DiCarlo JJ (2016) Explicit information for category-orthogonal object properties increases along the ventral stream. *Nat Neurosci* 19(4):613–622.

557 59. Hung CP, Kreiman G, Poggio T, DiCarlo JJ (2005) Fast Readout of Object Identity from
558 Macaque Inferior Temporal Cortex. *Science* 310(5749):863–866.

559 60. Riesenhuber M, Poggio T (1999) Hierarchical models of object recognition in cortex. *Nat*
560 *Neurosci* 2(11):1019–1025.

561 61. Crouzet SM, Kirchner H, Thorpe SJ (2010) Fast saccades toward faces: Face detection in just
562 100 ms. *J Vis* 10(4):16.

563 62. Honey C, Kirchner H, VanRullen R (2008) Faces in the cloud: Fourier power spectrum biases
564 ultrarapid face detection. *J Vis* 8(12):9–9.

565 63. Kirchner H, Thorpe SJ (2006) Ultra-rapid object detection with saccadic eye movements:
566 Visual processing speed revisited. *Vision Res* 46(11):1762–1776.

567 64. Thorpe S, Fize D, Marlot C (1996) Speed of processing in the human visual system. *nature*
568 381(6582):520–522.

569 65. Long B, Konkle T, Cohen MA, Alvarez GA (2016) Mid-level perceptual features distinguish
570 objects of different real-world sizes. *J Exp Psychol Gen* 145(1):95.

571 66. Kaiser D, Azzalini DC, Peelen MV (2016) Shape-independent object category responses
572 revealed by MEG and fMRI decoding. *J Neurophysiol* 115(4):2246–2250.

573 67. Ungerleider LG, Mishkin M (1982) Two cortical visual systems. *Anal Vis Behav*:549–586.

574 68. Sereno AB, Maunsell JHR (1998) Shape selectivity in primate lateral intraparietal cortex.
575 *Nature* 395(6701):500–503.

576 69. Silver MA, Kastner S (2009) Topographic maps in human frontal and parietal cortex. *Trends*
577 *Cogn Sci* 13(11):488–495.

578 70. Woolgar A, Golland P, Bode S (2014) Coping with confounds in multivoxel pattern analysis:
579 What should we do about reaction time differences? A comment on Todd, Nystrom & Cohen
580 2013. *NeuroImage* 98:506–512.

581 71. Hebart MN, Baker CI (2017) Deconstructing multivariate decoding for the study of brain
582 function. *NeuroImage*. doi:10.1016/j.neuroimage.2017.08.005.

583 72. Woolgar A, Jackson J, Duncan J (2016) Coding of Visual, Auditory, Rule, and Response
584 Information in the Brain: 10 Years of Multivoxel Pattern Analysis. *J Cogn Neurosci*
585 28(10):1433–1454.

586 73. Jackson J, Rich AN, Williams MA, Woolgar A (2016) Feature-selective Attention in
587 Frontoparietal Cortex: Multivoxel Codes Adjust to Prioritize Task-relevant Information. *J Cogn*
588 *Neurosci* 29(2):310–321.

589 74. Duncan J (2001) An adaptive coding model of neural function in prefrontal cortex. *Nat Rev*
590 *Neurosci* 2(11):820–829.

591 75. Freedman DJ, Assad JA (2016) Neuronal Mechanisms of Visual Categorization: An Abstract
592 View on Decision Making. *Annu Rev Neurosci* 39(1):129–147.

593 76. Jeong SK, Xu Y (2016) Behaviorally Relevant Abstract Object Identity Representation in the
594 Human Parietal Cortex. *J Neurosci* 36(5):1607–1619.

595 77. Bugatus L, Weiner KS, Grill-Spector K (2017) Task alters category representations in
596 prefrontal but not high-level visual cortex. *NeuroImage* 155:437–449.

597 78. Crouzet SM, Thorpe SJ (2011) Low-Level Cues and Ultra-Fast Face Detection. *Front Psychol* 2.
598 doi:10.3389/fpsyg.2011.00342.

599 79. Wu C-T, Crouzet SM, Thorpe SJ, Fabre-Thorpe M (2015) At 120 msec You Can Spot the Animal
600 but You Don't Yet Know It's a Dog. *J Cogn Neurosci* 27(1):141–149.

601 80. Pereira F, Mitchell T, Botvinick M (2009) Machine learning classifiers and fMRI: A tutorial
602 overview. *NeuroImage* 45(1, Supplement 1):S199–S209.

603 81. Grootswagers T, Wardle SG, Carlson TA (2017) Decoding Dynamic Brain Patterns from Evoked
604 Responses: A Tutorial on Multivariate Pattern Analysis Applied to Time Series Neuroimaging
605 Data. *J Cogn Neurosci* 29(4):677–697.

606 82. Oosterhof NN, Connolly AC, Haxby JV (2016) CoSMoMVPA: Multi-Modal Multivariate Pattern
607 Analysis of Neuroimaging Data in Matlab/GNU Octave. *Front Neuroinformatics*:27.

608 83. Benjamini Y, Hochberg Y (1995) Controlling the False Discovery Rate: A Practical and Powerful
609 Approach to Multiple Testing. *J R Stat Soc Ser B Methodol* 57(1):289–300.

610

611 **Figure and table legends**

612

613 **Figure 1. General experimental rationale.** Stimuli (**A,C**) used to map fMRI brain responses and
614 brain coverage (**B,C**) for fMRI study 1 and 2 respectively. **E**. Acquisition of reaction times on object
615 categorisation tasks. Reaction times for categorisation contrasts were collected in a different pool
616 of participants than the ones participating in the fMRI experiment. On each trial, a stimulus was
617 displayed for 250ms, and participants categorised it into two categories (exemplarily here:
618 animate vs inanimate) by pressing one of two keys. **F.** The two-partite approach to separately
619 localize decodable information and information that is suitable for read out in behaviour. For both
620 parts, a local cluster of neighbouring voxels (i.e., searchlight) was used to train a linear support
621 vector machine (SVM) on an image category classification task (e.g., animacy). To localize
622 decodable information, the classifier was tested on left-out data, storing the classification

accuracy at the centre voxel of the searchlight. To localise information that was suitably formatted for read-out in a categorisation task, the distances of objects to the classifier hyperplane were correlated with the reaction times for the same object images on the same classification task. Repeated for every voxel, this resulted for each subject in one map of decoding accuracies and one of correlations. For visualisation, significant correlation voxels were superimposed on significant decoding accuracy voxels, each showing group average values in significant voxels.

Figure 2. Relationship between decodable information and categorisation behaviour for animacy. A. In experiment 1, decodable animacy information (hot colours) was found throughout the ventral stream. A correlation between distance to the classifier boundary and reaction time for animate stimuli (cool colours) was found in a subset of these areas. **B.** The results of the analysis for experiment 2 corroborated these findings, and showed decodable information in prefrontal areas and in the dorsal visual stream. Correlations between distance and reaction time were also present in the dorsal stream. Visualizations show average results across subjects in significant voxels (N=15, sign-rank test, $p<0.05$ fdr-corrected) projected onto axial slices of a standard T_1 image in MNI space.

Figure 3. Quantifying the decodable information in visual areas and their contribution to categorisation behaviour. A. Locations of topographical ROIs of the visual system (47), containing early visual cortex (EVC) areas V1 and V2, mid-level areas V3 and hV4, high level ventral occipital (VO) and parahippocampal cortex (PHC), temporal occipital (TO) and lateral occipital (LO) areas, areas in the intra-parietal sulcus (IPS), the superior parietal lobule (SPL), and the frontal eye fields (FEF). **B-C.** The ratio between significant voxels in an ROI and the size of the ROI. Orange points show the ratio of voxels within the ROI that had significant animacy decoding performance. Blue points show the ratio of voxels with a significant correlation between distance to the hyperplane

648 and RT for 'animate'. The lower, middle and upper points on these lines indicate 5th, 50th, and 95th
649 percentiles (bootstrapping of participants 10,000 times). These results quantify the increasing
650 contribution of early to late areas in the ventral visual stream to animacy categorisation
651 behaviour.
652
653 **Figure 4. Relationship between decodable information and categorisation behaviour for face**
654 **versus body and food versus not food. A.** In experiment 1, decodable face versus body
655 information (hot colours) was found in the entire ventral stream. A distance-RT-correlation for the
656 face stimuli (cool colours) was found in a subset of these areas. **B.** In experiment 2, food versus
657 not food was decodable in some areas in the ventral visual stream. A distance-RT-correlation for
658 the 'not food' stimuli was found in a subset of these areas. Visualisations show average results
659 across subjects in significant voxels (N=15, sign-rank test, $p<0.05$ fdr-corrected) projected onto
660 axial slices of a standard T_1 image in MNI space.
661
662 **Table 1. Results for all categorisation contrasts.** For all categorisation contrasts, we report the
663 number of significant voxels (after correction for multiple comparisons), its peak value (maximum
664 for decoding or minimum for distance-RT-correlation) and uncorrected p-value, and the peak's
665 location in MNI-XYZ coordinates.
666

Figure 1

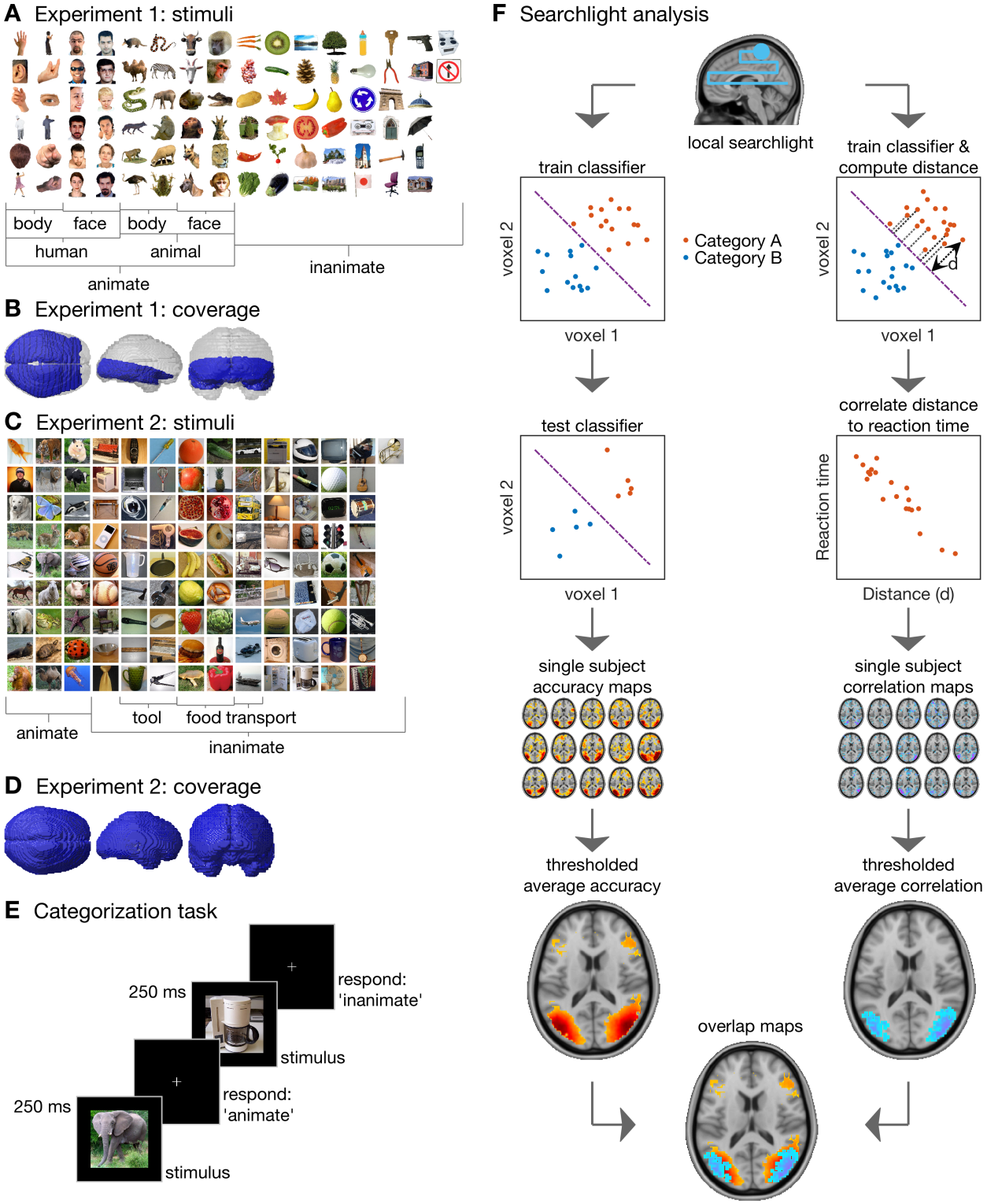
A Experiment 1: stimuli
body
face
body
face
human
animal
animate
inanimate
B Experiment 1: coverage
C Experiment 2: stimuli
animate
tool
food
transport
inanimate
D Experiment 2: coverage
E Categorization task
250 ms
respond: 'inanimate'
stimulus
250 ms
respond: 'animate'
stimulus
F Searchlight analysis
local searchlight
train classifier
voxel 2
voxel 1
Category A
Category B
train classifier & compute distance
d
test classifier
correlate distance to reaction time
Reaction time
Distance (d)
single subject accuracy maps
single subject correlation maps
thresholded average accuracy
thresholded average correlation
overlap maps

Figure 2

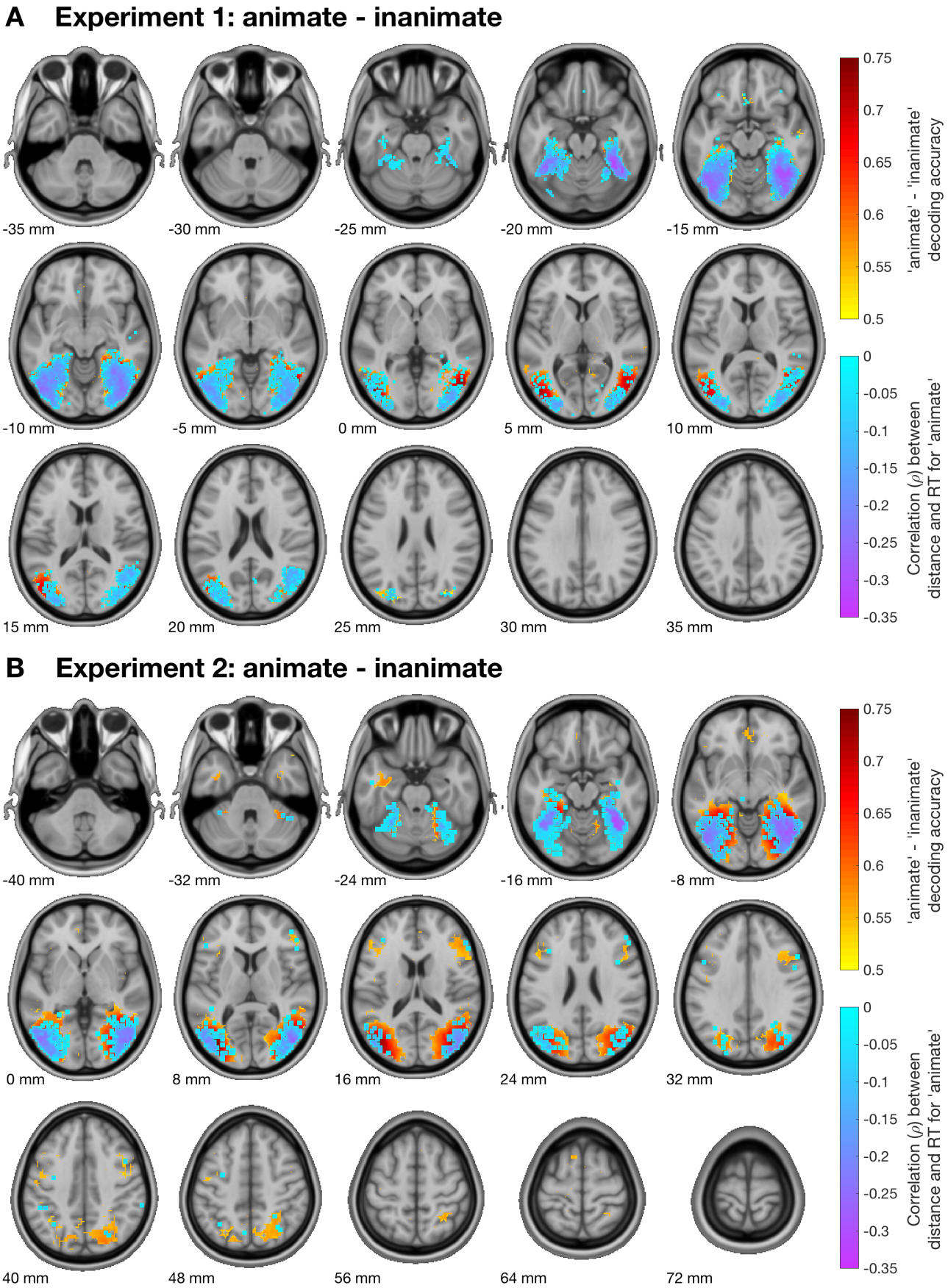
A Experiment 1: animate - inanimate
-35 mm
-30 mm
-25 mm
-20 mm
-15 mm
-10 mm
-5 mm
0 mm
5 mm
10 mm
15 mm
20 mm
25 mm
30 mm
35 mm
0.75
0.7
0.65
0.6
0.55
0.5
'animate' - 'inanimate' decoding accuracy
0
-0.05
-0.1
-0.15
-0.2
-0.25
-0.3
-0.35
Correlation (ρ) between distance and RT for 'animate'
B Experiment 2: animate - inanimate
-40 mm
-32 mm
-24 mm
-16 mm
-8 mm
0 mm
8 mm
16 mm
24 mm
32 mm
40 mm
48 mm
56 mm
64 mm
72 mm
0.75
0.7
0.65
0.6
0.55
0.5
'animate' - 'inanimate' decoding accuracy
0
-0.05
-0.1
-0.15
-0.2
-0.25
-0.3
-0.35
Correlation (ρ) between distance and RT for 'animate'

673 **Figure 3**

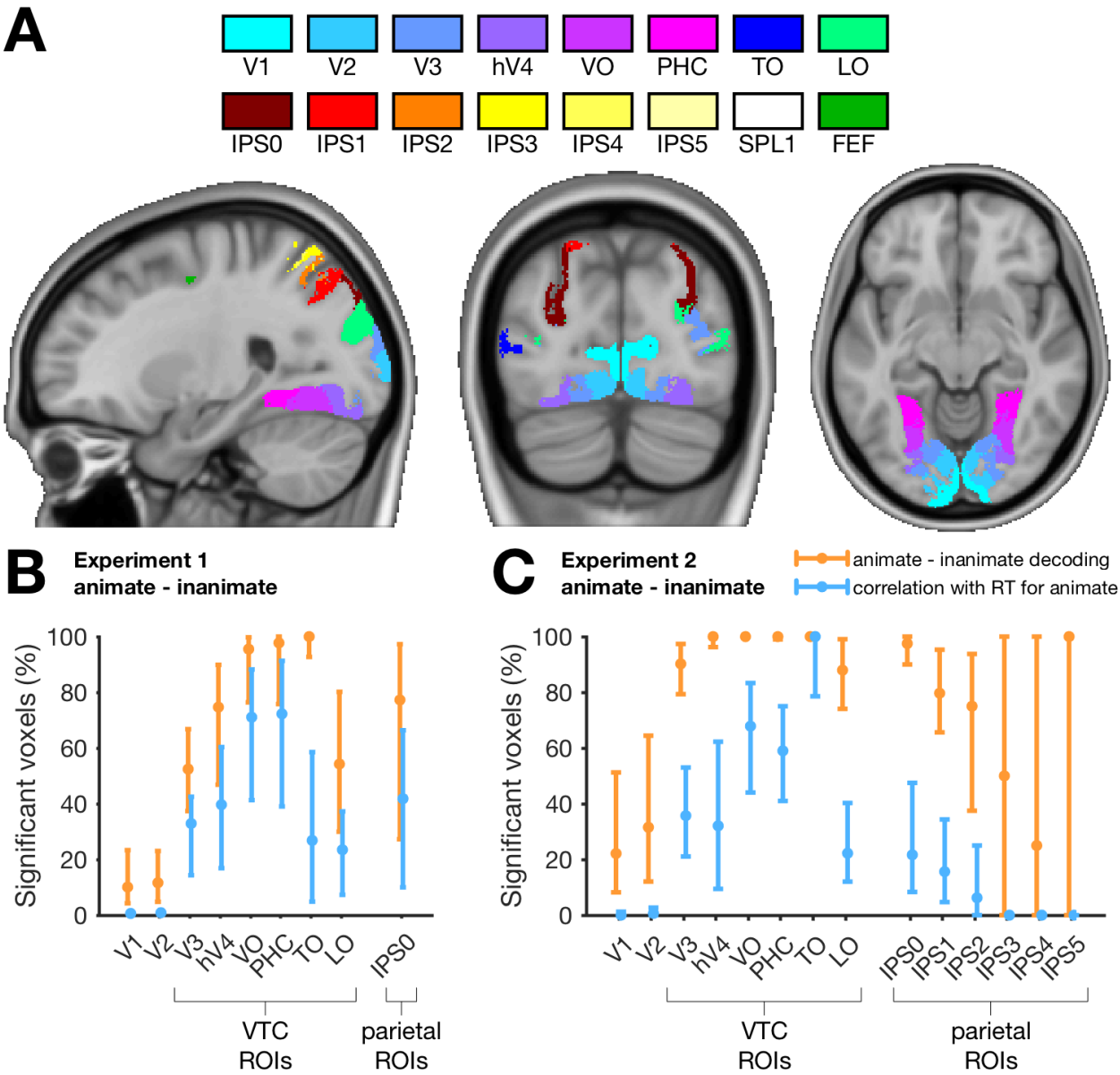

674

675

Figure 4

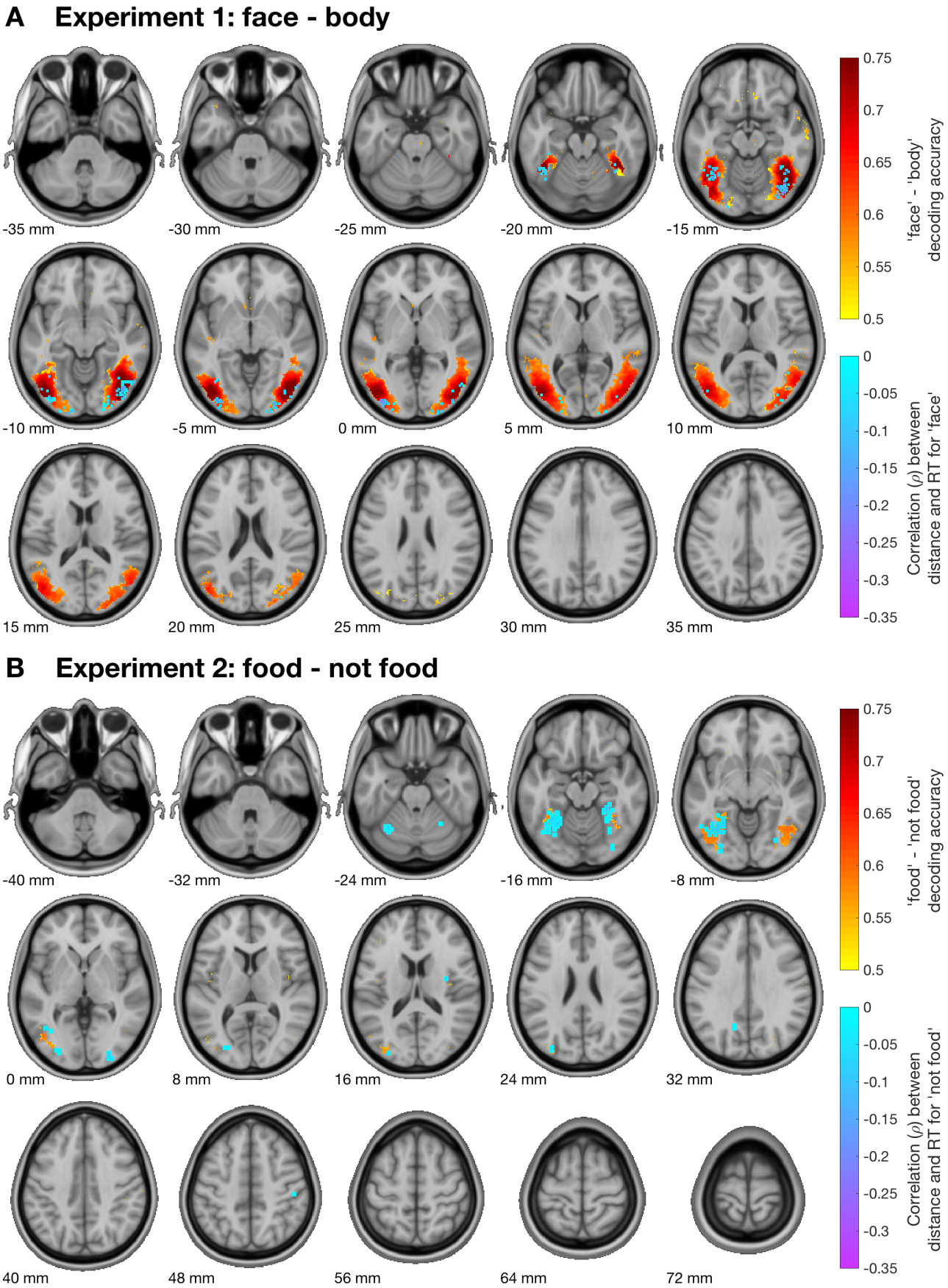
A Experiment 1: face - body
-35 mm
-30 mm
-25 mm
-20 mm
-15 mm
-10 mm
-5 mm
0 mm
5 mm
10 mm
15 mm
20 mm
25 mm
30 mm
35 mm
0.75
0.7
0.65
0.6
0.55
0.5
'face' - 'body' decoding accuracy
0
-0.05
-0.1
-0.15
-0.2
-0.25
-0.3
-0.35
Correlation (ρ) between distance and RT for 'face'
B Experiment 2: food - not food
-40 mm
-32 mm
-24 mm
-16 mm
-8 mm
0 mm
8 mm
16 mm
24 mm
32 mm
40 mm
48 mm
56 mm
64 mm
72 mm
0.75
0.7
0.65
0.6
0.55
0.5
'food' - 'not food' decoding accuracy
0
-0.05
-0.1
-0.15
-0.2
-0.25
-0.3
-0.35
Correlation (ρ) between distance and RT for 'not food'

Table 1

Contrast	#significant voxels	Max/min	uncorr. p-value	X	Y	Z
A) decoding 'animate' vs 'inanimate' (exp 1)	11745	0.80	0.0000	36	-52	-15
Distance-RT-correlation 'animate'	6410	-0.38	0.0000	38	-58	-19
Distance-RT-correlation 'inanimate'	0	-0.16	0.0021	-48	-58	5
B) decoding 'human' vs 'animal'	4863	0.69	0.0000	22	-90	-13
Distance-RT-correlation 'human'	0	-0.29	0.0002	30	-58	-15
Distance-RT-correlation 'animal'	0	-0.17	0.0072	48	-46	-4
C) decoding 'face' vs 'body'	10661	0.84	0.0000	44	-78	-10
Distance-RT-correlation 'face'	226	-0.32	0.0000	40	-76	-15
Distance-RT-correlation 'body'	0	-0.20	0.0000	-54	-68	16
D) decoding 'animate' vs 'inanimate' (exp 2)	8824	0.80	0.0000	36	-55	-11
Distance-RT-correlation 'animate'	2015	-0.34	0.0000	51	-73	-2
Distance-RT-correlation 'inanimate'	0	-0.12	0.0002	-21	-43	-2
E) decoding 'tool' vs 'not tool'	0	0.58	0.0002	-30	-94	7
Distance-RT-correlation 'tool'	0	-0.25	0.0013	-33	-13	19
Distance-RT-correlation 'not tool'	0	-0.24	0.0001	-33	-52	-17
F) decoding 'transport' vs 'not transport'	0	0.59	0.0001	33	-94	1
Distance-RT-correlation 'transport'	0	-0.32	0.0003	15	50	4
Distance-RT-correlation 'non-transport'	0	-0.18	0.0000	-33	-55	-14
G) decoding 'food' vs 'not food'	1092	0.62	0.0002	36	-55	-14
Distance-RT-correlation 'food'	0	-0.16	0.0177	-18	26	-5
Distance-RT-correlation 'not food'	154	-0.13	0.0002	27	-40	-14